

## Astrometric Measurements of Four Physical Double Star Systems

Corbin Breeden, Zoe Schurman, Michael Pylypovych, Atria Freeman, Kalée Tock  
Stanford Online High School, Redwood City, California; corbin.breeden@gmail.com

### Abstract

Images of four Washington Double Star systems, WDS 06065-4705 TVB 115, WDS 06404+1423 TVB 139, WDS 08494-1711 POC 3, and WDS 10019+7334 STF 1393 were taken and reduced in AstroImageJ to evaluate the position angle and separation, current for 2024.0. The resulting astrometric measurement is presented, along with a historical data plot and a comparison of relative three-dimensional space velocity to system escape velocity. All four systems are found to exhibit common proper motion, meaning they are moving in almost the same way. The data plot and measurements, combined with the Gaia Data Release 3 information suggest that TVB 115 could be a gravitationally bound binary star system, while TVB 139, POC 3, and STF 1393 are physical double star systems.

### 1. Introduction

Binary star systems fall under the umbrella term of a “physical” system, which move together in space but may or may not be gravitationally bound and in orbit around one another. While binary systems receive substantial focus, other types of physical relationships between stars are just as intriguing. Physically related stars often share an origin, and studying the nature of these relationships and origins can indirectly inform us about the nature of this galaxy and its history. The following paper investigates the physicality of four double star systems.

When selecting targets from the Washington Double Star (WDS) catalog, several parameters were employed. First, the target needed to have an RA between 5 and 13 hours so it would be visible in midwinter when observations were to be made. Second, the secondary star’s magnitude needed to be less than 13, to ensure both stars would be bright enough to be resolved on a Complementary Metal-Oxide Semiconductor (CMOS) image with 0.35 m telescopes. The third requirement was a difference in magnitude ( $\Delta\text{mag}$ ) of less than 3. If the star system had a  $\Delta\text{mag}$  greater than 3, it would be challenging to capture both stars in the system in the same image. Fourth, the two stars needed to have a separation between 5 and 15 arcseconds. A double star system with a separation of less than 5" would not be easily resolved, due to the closeness of the two stars in the image. Systems with a separation of greater than 15" are less likely to have a strong physical relationship. The final parameter was that the star system needed to be classified as a physical double. Ultimately, the systems TVB 115, TVB 139, POC 3, and STF 1393 were selected.

To find the spectral classes of the stars in each system, we used the measurements from Gaia DR 3 about their BP-RP color and Gaia G-filter magnitude corrected for parallax (absolute G magnitude). These measurements were used to plot the star on Gaia’s Hertzsprung-Russell Diagram (Babusiaux, 2023; Prusti, 2016; Vallenari, 2023). The stars’ positions on this diagram were then used to estimate their spectral types

and corresponding masses (Morgan, S. 2023; Mamajek, 2022). Figure 1 shows the stars' HR-diagram positions; Table 1 shows the data used to plot those positions, plus the resulting mass estimates. All four systems are listed as "physical" in Stelle Doppie and are located in winter constellations: TVB 115 and POC 3 in Puppis, TVB 139 in Gemini, and STF 1393 in Draco.

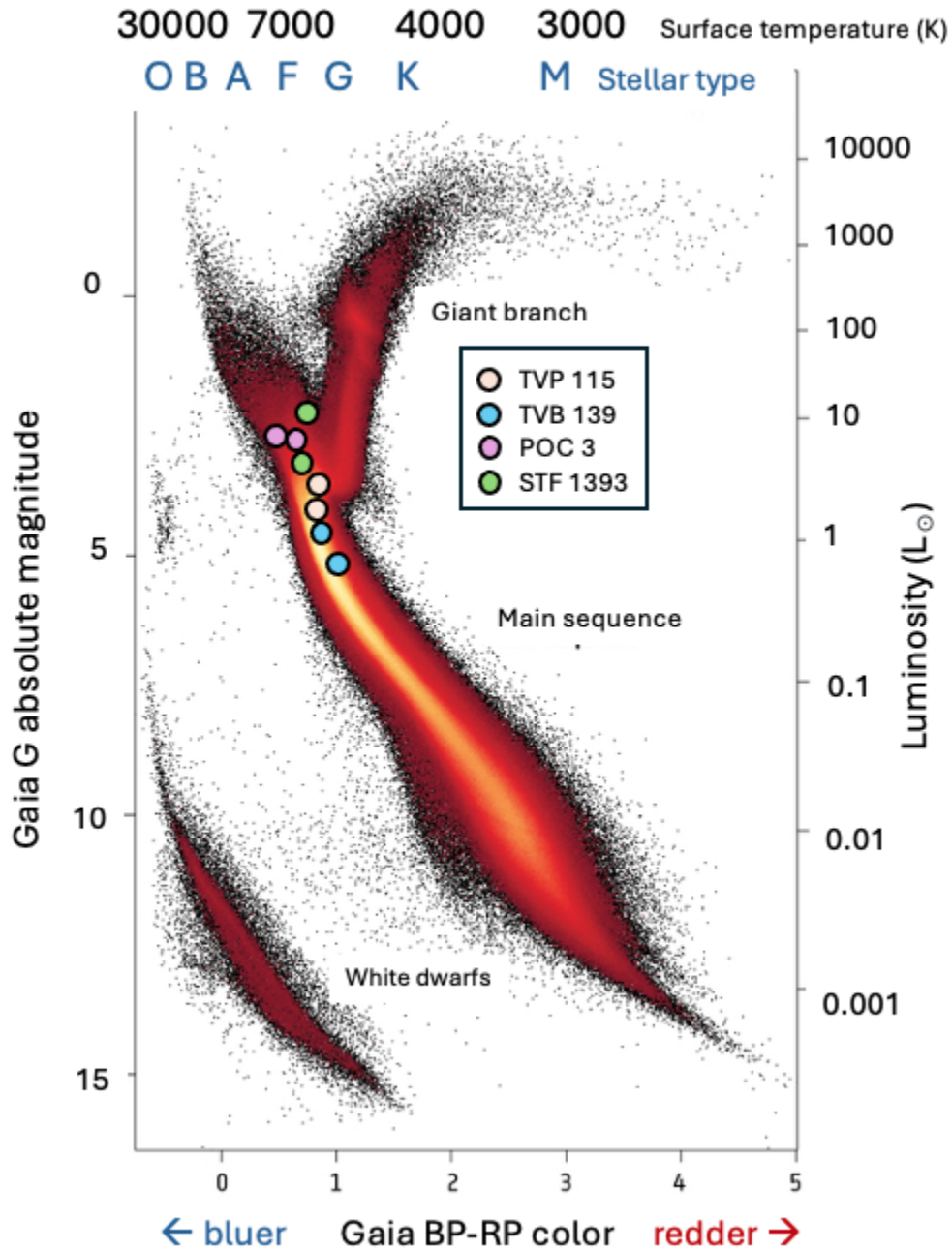


Figure 1: Gaia CMD diagram with each system's stars plotted according to their Gaia G absolute magnitude and Gaia BP-RP color

Table 1. Coordinate, Magnitude, Colors, and Estimated Masses.

System	Coordinates	Absolute Gaia Gmag (Primary)	Absolute Gaia Gmag (Secondary)	Colors (Bp-Rp) Primary	Color (Bp-Rp) Secondary	Primary Est. Mass (Solar Masses)	Secondary Est. Mass (Solar Masses)
TVB 115	06h 06m 29.06s -47° 05' 08.7"	3.80	4.13	0.86044	0.83652	0.9	1.1
TVB 139	06h 40m 22.89s +14° 23' 16.5"	4.52	5.24	0.84646	0.83931	1.5	0.8
POC 3	08h 49m 22.61s -17° 11' 29.6"	3.06	3.37	0.57963	0.69653	1.4	1.4
STF 1393	10h 01m 56.54s +73° 34' 07.1"	3.80	4.14	0.70094	0.64310	1.2 <sup>1</sup>	1.6

<sup>1</sup>The primary star for STF 1393 has a spectral type of F8 (Brandt, 2021), implying a mass of 1.2 solar masses. It is the only star for which there is a known spectral type.

## 2. Instruments Used

All images were taken by a Planewave Delta Rho 350 + QHY600 CMOS camera. The telescope has an aperture of 0.35m and a focal length of 1050mm. The QHY600 CMOS camera has an angular pixel size of 0.73", and an FOV of 1.9° x 1.2°, cut down to 30' x 30' for the default imaging "central mode" of these Las Cumbres Observatory Global Telescope (LCOGT) instruments. Two different LCOGT sites were used: Teide and Siding Spring. The LCOGT Teide Observatory Aqawan A #1 is located on the island of Tenerife in Spain's Canary Islands, at an altitude of 2390m. The LCOGT Siding Spring Observatory is in Coonabarabran, New South Wales, Australia, at an altitude of 1164m. The two filters used were Bessell-V and PanSTARRS-w (Bessell, 1990; Tonry, 2012). Date of observation, exposure time, images taken, and filter used are shown in Table 2.

Table 2. Observation data for the set of double star systems.

System	LCOGT Observatory	Decimal Date of Observation	Images Taken	Exposure Time (sec)	Filter Used
TVB 115	Siding Spring	2024.0329	10	30	Bessell-V
TVB 139	Teide	2024.0192	11	25	PanSTARRS-w
POC 3	Teide	2024.0301	10	5	Bessell-V
STF 1393	Teide	2024.0301	10	8.75	Bessell-V

### 3. Measurements

All images for TVB 115, TVB 139, and STF 1393 were well-resolved, with clearly separated stars and minimal blurring. Images of POC 3 initially seemed to have stars blended together, but after adjusting brightness and contrast, the stars were well defined. Additionally, while TVB 115 has a smudge next to it, this third star is not in the system - according to Gaia data, it has a parallax far different from TVB 115. Measurements were made with AstroImageJ's multi-aperture photometry tool. Examples of the measurement process for each system are shown in Figure 2. The individual measurements of position angle in degrees and separation in arcseconds can be found in Appendix A.

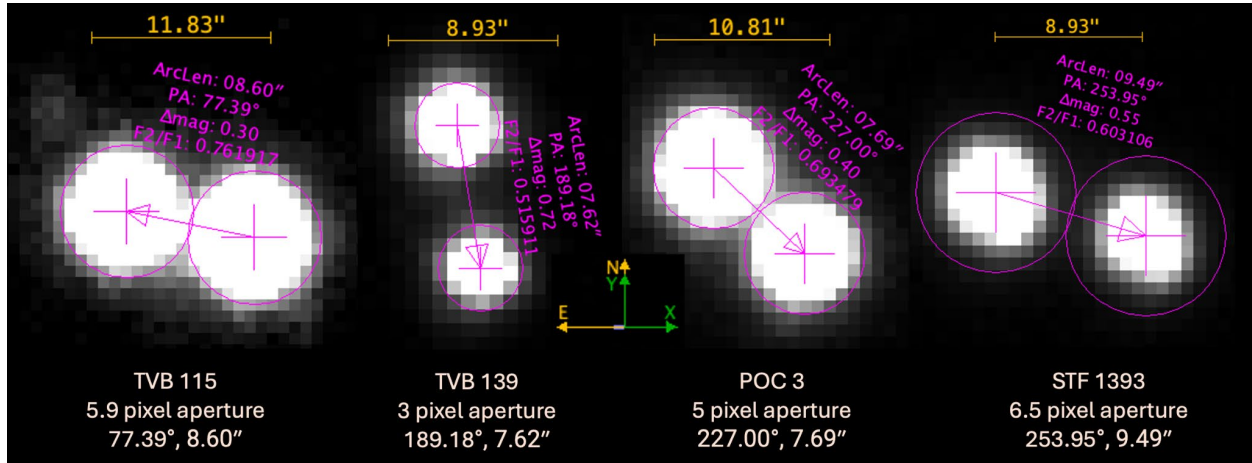


Figure 2: Example of the measurement process for each system

The individual measurements of the images were averaged, with average position angle and separation and accompanying standard errors depicted in Table 3.

Table 3. Average measurements, standard deviation, and standard error of the mean average.

System	Position Angle (°)	Standard Deviation on PA (°)	Standard Error PA (°)	Separation (")	Standard Deviation Separation (")	Standard Error Separation (")
TVB 115	77.1	0.48	0.17	8.56	0.116	0.041
TVB 139	189.2	0.07	0.02	7.63	0.023	0.007
POC 3	227.3	0.24	0.08	7.72	0.044	0.014
STF 1393	254.1	0.22	0.07	9.47	0.023	0.007

#### 4. Results and Discussion

To assess the radial proximity of the stars in each pair to each other and the degree to which their motion is synchronized, Gaia DR3 parallax and proper motion measurements are tabulated in Table 4. The proper motion ratio (rPM) is calculated by taking the ratio of the magnitude of the relative proper motion vector to the magnitude of the longer proper motion vector of the two stars (Harshaw, 2016). Double star systems are considered to display common proper motion if the rPM value is less than 0.2, as all of these are.

Table 4. Parallax and proper motion data for the set of double star systems, including the proper motion ratio (rPM). Data taken from Gaia DR3.

System	Parallax of Primary (mas)	Parallax of Secondary (mas)	Proper Motion of Primary (mas/yr)	Proper Motion of Secondary (mas/yr)	rPM
TVB 115	$2.89 \pm 0.011$	$2.90 \pm 0.011$	$(-9.97 \pm .01, -6.2 \pm .01)$	$(-9.97 \pm .01, -6.17 \pm .01)$	0.001
TVB 139	$2.92 \pm 0.014$	$2.94 \pm 0.023$	$(12.1 \pm 0.02, -27.4 \pm 0.02)$	$(12.5 \pm 0.03, -27.04 \pm 0.03)$	0.017
POC 3	$5.77 \pm 0.014$	$5.96 \pm 0.024$	$(1.00 \pm 0.01, -33.9 \pm 0.01)$	$(0.68 \pm 0.02, -34.3 \pm 0.02)$	0.015
STF 1393	$2.81 \pm 0.014$	$2.81 \pm 0.015$	$(14.02 \pm 0.01, -7.0 \pm 0.02)$	$(15.8 \pm 0.02, -7.4 \pm 0.02)$	0.106

One study which included POC 3 (identifier HD 75423) concluded that stars with  $>1$  parsec (pc) separation cannot be easily distinguished as genuine wide binaries (binary systems set relatively far apart) instead of moving groups, contamination from randomly aligned stars, or ionized former binary systems (former binaries that have become gravitationally unbound). The study instead suggests that stars with  $<1$  pc separation are high-confidence candidates for being a binary (Andrews, et al., 2017). The three-dimensional separation of POC 3 is calculated using the separation and the parallaxes of the stars and is greater than 5 pc, so POC 3 is unlikely to be gravitationally bound according to the Andrews criterion. Despite likely not being gravitationally bound, POC 3 shows common proper motion even at  $>5$  pc separation.

The three remaining systems have both common proper motion and similar parallaxes between their two stars, suggesting a stronger physical relationship.

Another way to assess the physical relationship of double star systems is the comparison of system escape velocity to relative three-dimensional space velocity. The stars in a system whose three-dimensional space velocity is less than the system escape velocity are likely to be gravitationally bound. We calculated system escape velocity (in m/s) using the following equation:

$$v_{escape} = \sqrt{\frac{2G(m_1 + m_2)}{r}}$$

where  $m_1$  is the estimated mass of the primary star,  $m_2$  is the estimated mass of the secondary star, and  $G$  is the gravitational constant. In this equation, the variable  $r$  is *either* the transverse separation in space when the stars' parallaxes overlap within uncertainty *or*  $r$  is the three-dimensional spatial separation when the stars' parallaxes do not overlap within uncertainty (Bonifacio 2022). Transverse separation (in parsecs) is calculated using the following equation:

$$Sep_{pc} = \frac{Sep_{arcseconds} \times \frac{1deg}{3600''} \times \frac{2\pi rad}{360deg}}{parallax''}$$

Three-dimensional spatial separation (in parsecs) is calculated by converting the parallaxes into parsecs and taking the difference in radial distance between the two stars, then applying the Pythagorean Theorem to the transverse separation and radial separation to account for all three dimensions. POC 3 was the only system whose stars' parallaxes do not overlap within uncertainty, necessitating use of the three-dimensional spatial separation when calculating the escape velocity.

To find the relative three-dimensional space velocity to compare with the system escape velocity, we again applied the Pythagorean Theorem to the relative transverse motion through space and the relative radial motion through space. The relative transverse motion through space (in m/s) was found by dividing the magnitude of the relative proper motion vector by the parallax of the primary star (this assumes that the two stars are close to the same distance from Earth). The relative radial motion through space (in m/s) was calculated by taking the absolute value of the difference between the Gaia primary and secondary radial velocities when given. POC 3 was the only system for which Gaia did not have a radial velocity value for the secondary star, so relative space velocity was taken to be the same as the relative transverse motion through space. Masses were roughly estimated with Gaia BP-RP values and Gaia G magnitude values, or with the spectral type if it was known, as described previously and listed in Table 1. The relative and escape velocities computed as described here are presented in Table 5.

Table 5. Separation calculations, system escape velocity, and relative space velocity.

System	Transverse separation (pc)	System escape velocity (m/s)	Gaia radial velocity of primary (km/s)	Gaia radial velocity of secondary (km/s)	Transverse velocity (m/s)	Relative 3D space velocity (m/s)
TVB 115	0.014	1065	25.22	25.70	14	488
TVB 139	0.013	1243	108.76	106.71	842	2217
POC 3	5.78'	65	-13.32	N/A	423	423
STF 1393	0.017	1196	-47.95	-49.25	3118	3380

<sup>1</sup>The italicized transverse separation for POC 3 indicates the three-dimensional spatial separation that incorporates transverse and radial separation, used when the stars' parallaxes do not overlap with uncertainty. The three-dimensional spatial separation was used to calculate the system escape velocity for POC 3 only. The other systems used transverse separation.

Having estimated the system escape velocity, we compared it to the calculated relative three-dimensional space velocity. TVB 115 has a relative space velocity less than its system escape velocity suggesting that the stars may be gravitationally bound. For TVB 139 and STF 1393, the escape and relative velocities are the same order of magnitude, which problematizes a definitive conclusion. For POC 3, however, the relative space velocity is more than six times greater than the escape velocity, as might be expected for a system whose components are so widely separated.

While POC 3's components likely have a weaker physical relationship, the spectral type analysis paper from Houk and Smith-More in 1988 suggests that the secondary star in POC 3 may itself have a very faint companion of Type G or K. When POC 3's coordinates are queried in both Simbad and Gaia DR3, three stars appear. The Gaia DR3 listing appears in Figure 3. Because Gaia's angular resolution limit is 0.4 arcseconds, and the difference between the secondary and possible tertiary star in Simbad is less than 0.4 arcseconds, Gaia was not able to accurately resolve the third star, which explains the lack of color, parallax, proper motion, and other data points (Luri, 2018). The Gaia DR3 listed G magnitude of 20.44 explains why the possible third star does not appear in any images. Further measurements and analyses of POC 3 are recommended to better describe this possible third star.

The 10 closest stars in order of proximity to 08h49m22.61-17d11m29.6s are:

PA	Sep	Gmag	Color	Plx	ePlx	pmra	epmra	pmdec	epmdec
164.37777	0.51042	9.17912	0.57963	5.96423	0.01426	1.00494	0.01292	-33.91991	0.01328
344.94487	5.21541	20.4426	--	--	--	--	--	--	--
227.13756	7.75106	9.56644	0.69653	5.76561	0.02434	0.67755	0.02303	-34.33953	0.02341

Figure 3: Gaia DR3 listing for POC 3 with the primary star in the first row, secondary star in the third row, and possible tertiary star in the second row with many data points missing

## 5. Plots

Using historical position angle and separation data obtained from the United States Naval Observatory, as well as Gaia DR3 measurements and our measurements, the positions of the secondary stars with the primary stars at the origins over time are plotted in Figure 4.

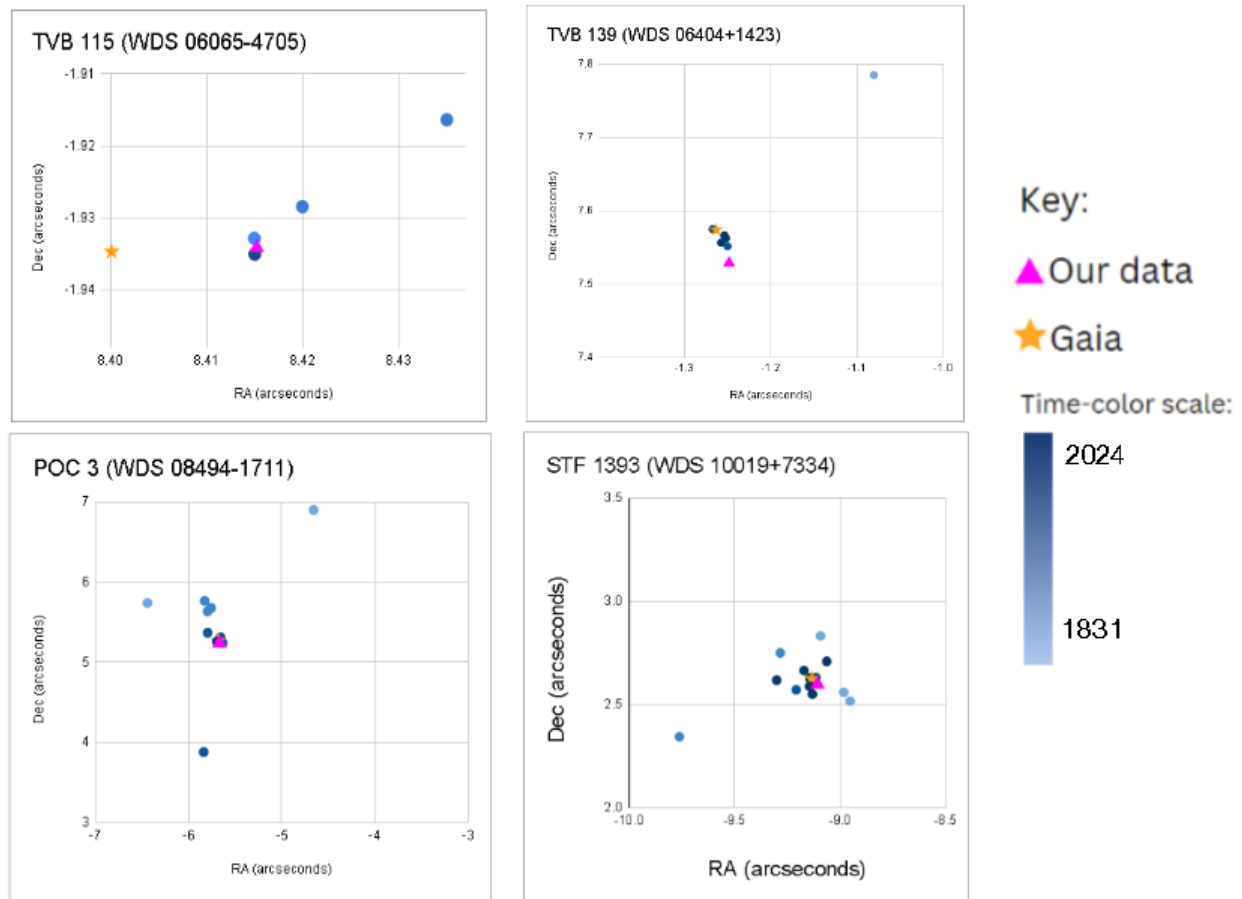


Figure 4: Position of secondary star in RA and Dec of TVB 115, TVB 139, POC 3, STF 1393 with respect to primary with labeled measurements from Gaia and this study. The first two data points of TVB 115 from 1902.94 are out-of-bounds at (8.05, -2.07) and (8.58, -1.81). The first data point of STF 1393 from 1831.84 is out-of-bounds at (-11.69, 2.70)

The data plotted above is from the historical data requested from the Washington Double Star Catalog. None of these systems have a published orbit or linear solution. Despite the fact that the component stars of TVB 115 have a lower relative velocity than escape velocity, the erratic temporal dependence of the data in Figure 4 does not suggest an orbital solution.

The historical data plot of TVB 139 differs in general shape from the plots of TVB 115, POC 3, and STF 1393. We propose that the outlier at (-1.08, 7.78) in TVB 139 be deprioritized as it is from the oldest known measurement and could therefore be subject to more uncertainty than the more recent ones. The graph of TVB 139 is unique in its shape because it shows promising signs of a curve relative to the origin. TVB 139 is worth further study to assess whether this trend continues.

There appears to be a lack of a trend over time in systems POC 3 and STF 1393. In POC 3, the distribution for historical data points in POC 3 is erratic and is likely to have no association between time and data points. It is important to note that the purple triangle representing the observations done in this study on POC 3 is obscuring the orange star corresponding to the Gaia data point in the graph. There is a similar

story in STF 1393. The first data point from 1831 is off the graph to the upper left, the furthest left visible point is the 6th observation from 1930. Meanwhile, the two furthest right points are from 1894 (-8.95, 2.52) and 1911(-8.98, 2.55). Furthermore, the 2015 Gaia DR3 data point is clumped in the middle of the graph along with the most recent 2024 data point. Both a fitted 2nd degree polynomial trendline that includes the out-of-bounds data point and the same trendline that only includes the visible data points fail to encompass the origin.

## 6. Conclusion

The measurements within this study were consistent with historical observations of the four systems. All four stars have common proper motion, classifying them as physical systems. Systems TVB 115 and STF 1393 could have long-period orbital solutions that don't show up in the timespan of the observations conducted so far. Based on escape velocity calculations, TVB 115 is the likeliest candidate for a long-period orbital solution. However, TVB 139 is the only system that shows some indication of curvature in the historical data plot. With the exception of TVB 115, the systems have escape velocities lower than their relative space velocity, implying that they are not gravitationally bound, though the data is significantly less conclusive for TVB 139 and STF 1393 and does not fully rule out the idea of any of these systems being binary. Given the parallax of the stars in POC 3 ( $>5$  pc), the system is unlikely to be gravitationally bound. Further observation is recommended for all four of these physical double star systems.

## Acknowledgements

This research was made possible by the Washington Double Star catalog maintained by the U.S. Naval Observatory, the Stelle Doppie catalog maintained by Gianluca Sordiglioni, Astrometry.net, and AstroImageJ software which was written by Karen Collins and John Kielkopf.

This work has made use of data from the European Space Agency (ESA) mission Gaia (<https://www.cosmos.esa.int/gaia>), processed by the Gaia Data Processing and Analysis Consortium (DPAC, <https://www.cosmos.esa.int/web/gaia/dpac/consortium>). Funding for the DPAC has been provided by national institutions, in particular the institutions participating in the Gaia Multilateral Agreement.

This work makes use of observations taken by the Planewave Delta Rho 350 + QHY600 CMOS camera systems of Las Cumbres Observatory Global Telescope Network located in Tenerife, Spain.

The Las Cumbres Observatory's education network telescopes were upgraded through generous support from the Gordon and Betty Moore Foundation.

This research has made use of the SIMBAD database, operated at CDS, Strasbourg, France (Wenger et al. 2000).

## References

- Andrews, J. J., Chanamé, J., & Agüeros, M. A. (2017). Wide binaries in Tycho-Gaia: search method and the distribution of orbital separations. *Monthly Notices of the Royal Astronomical Society*, 675–699. <https://doi.org/10.1093/mnras/stx2000>
- Bessell, M. S (1990). Publications of the Astronomical Society of the Pacific, 102, 1181-1199. <https://adsabs.harvard.edu/full/1990PASP..102.1181B>
- Brandt, T. D (2021). The Hipparcos-Gaia Catalog of Accelerations: Gaia EDR3 Edition. The Astrophysical Journal Supplemental Series, 254(2). <https://simbad.cds.unistra.fr/simbad/sim-ref?bibcode=2021ApJS..254...42B>
- Bonifacio, B., C. Marchetti, R. Caputo, and K. Tock. (2020). Measurements of Neglected Double Stars. *Journal of Double Star Observations*, 16(5), 411–423. [http://www.jdso.org/volume16/number5/Bonifacio\\_411\\_423.pdf](http://www.jdso.org/volume16/number5/Bonifacio_411_423.pdf)
- Evans, D. W, et. al (2018). Gaia Data Release 2 - Photometric content and validation. *A&A* 616, A4. [https://www.aanda.org/articles/aa/full\\_html/2018/08/aa32756-18/aa32756-18.html](https://www.aanda.org/articles/aa/full_html/2018/08/aa32756-18/aa32756-18.html)
- Gaia Collaboration, A. Vallenari, A. G. A. Brown, et al. (2022k). Gaia Data Release 3: Summary of the content and survey properties. arXiv e-prints, <https://arxiv.org/abs/2208.00211>
- Gaia Collaboration, C. Babusiaux, F. Van Leeuwen, et al. (2018). Gaia Data Release 2: Observational Hertzsprung-Russell diagrams. *A&A* 616, A10. [https://www.aanda.org/articles/aa/full\\_html/2018/08/aa32843-18/aa32843-18.html](https://www.aanda.org/articles/aa/full_html/2018/08/aa32843-18/aa32843-18.html)
- Gaia Collaboration, T. Prusti, J.H.J. de Bruijne, et al. (2016b). The Gaia mission. *A&A* 595, A1. [https://www.aanda.org/articles/aa/full\\_html/2016/11/aa29272-16/aa29272-16.html](https://www.aanda.org/articles/aa/full_html/2016/11/aa29272-16/aa29272-16.html)
- Gaia Collaboration, X. Luri, A. G. A. Brown, et al. (2018). Gaia Data Release 2: Using Gaia Parallaxes/ arXiv e-prints, <https://arxiv.org/abs/1804.09376>
- Harshaw, Richard (2016). CCD Measurements of 141 Proper Motion Stars: The Autumn 2015 Observing Program at the Brilliant Sky Observatory, Part 3. *Journal of Double Star Observations*, 12(4), 394–399. [http://www.jdso.org/volume12/number4/Harshaw\\_394\\_399.pdf](http://www.jdso.org/volume12/number4/Harshaw_394_399.pdf)
- Mamajek, E. (2022). A Modern Mean Dwarf Stellar Color and Effective Temperature Sequence. Department of Physics and Astronomy: University of Rochester. [https://www.pas.rochester.edu/~emamajek/EEM\\_dwarf\\_UBVIJHK\\_colors\\_Teff.txt](https://www.pas.rochester.edu/~emamajek/EEM_dwarf_UBVIJHK_colors_Teff.txt)
- Morgan, S. (Jan. 2023). Spectral Type Characteristics. <https://sites.uni.edu/morgans/astro/course/Notes/section2/spectraltemps.html>
- Tonry, J.L. et al. (2012). The Pan-STARRS1 Photometric System. *The Astrophysical Journal*, 750(2), 99. <https://iopscience.iop.org/article/10.1088/0004-637X/750/2/99/pdf>
- Wenger, M. et al. (Apr. 2000). “The SIMBAD astronomical database. The CDS reference database for astronomical objects”. In: *Astronomy and Astrophysics Supplement* 143, pp. 9–22. DOI: 10.1051/aas: 2000332. arXiv: astro-ph/0002110 [astro-ph].

**Appendix A:**

Table 6. Measurements from image reductions for each image and system.

PA for TVB 115 (°)	Sep for TVB 115 (")	PA for TVB 139 (°)	Sep for TVB 139 (")	PA for POC 3 (°)	Sep for POC 3 (")	PA for STF 1393 (°)	Sep for STF 1393 (")
76.46	8.51	189.18	7.62	227.00	7.69	253.95	9.49
77.93	8.65	189.27	7.61	227.04	7.72	254.12	9.48
76.58	8.8	189.1	7.62	227.06	7.73	254.32	9.48
76.79	8.51	189.23	7.63	227.36	7.72	254.15	9.47
76.96	8.55	189.17	7.62	227.55	7.72	253.96	9.44
77.1	8.36	189.07	7.64	227.37	7.62	253.83	9.48
76.95	8.55	189.16	7.63	227.34	7.78	253.93	9.49
77.85	8.59	189.06	7.69	226.87	7.71	254.07	9.48
77.04	8.62	189.18	7.61	227.57	7.75	253.87	9.47
76.87	8.49	189.17	7.62	227.38	7.76	254.56	9.42
		189.07	7.65				